Effect of Chromium Additions on the Mechanical and Physical Properties and Microstructure of Fe-Co-Ni-Cr-Mo-C Ultra-High Strength Steel: Part I

P. Machmeier, T. Matuszewski, R. Jones, and R. Ayer

The effect of chromium additions to an Fe-14Co-10Ni-0.1Mo-0.16C (AF1410 based) secondary hardening steel was evaluated by mechanical and physical properties and by microstructural examination. This unique behavior was extended to encompass a large range of aging temperatures and times that may be encountered during commercial thermal treatment and/or welding. In the aging range of 482 to 550 °C, an increase in chromium from 2 to 3% in the AF1410 based steel resulted in a substantial strength decrease concomitant with an increase in toughness. This behavior is related to a peak hardening shift, early M_2C carbide coarsening, and an increase in reverted austenite for the 1 wt% Cr increase. The increased aging kinetics resulting from the 3Cr steel caused a faster dissolution of Fe_3C and rapid changes in chromium partitioning in the $(Mo,Cr)_2C$ carbide resulting in a coherency loss with a corresponding decrease in lattice parameter. The kinetics of the secondary hardening reaction, for the two steels, was determined by resistivity data for changes in aging parameters (time/temperature).

Keywords
mechanical properties, steel properties, ultra high strengh steels

1. Introduction

THE PHENOMENA of secondary hardening in alloy steels, with the replacement of cementite by alloy carbides during the aging reaction, has been recognized for a long time (Ref 1, 2). Numerous investigations were conducted on the M_2C precipitation mechanism (Ref 3-5); however, these systems were not candidates for high performance structural steel because the strength and toughness relationships were not optimized. Early investigations by Chandhok et al. (Ref 6, 7) disclosed that cobalt increased the activity of carbon and resulted in a higher dislocation density in ferrite. Later, Speich et al. (Ref 8) also reported the retardation of a highly dislocated substructure in Fe-Ni-Co-Cr-Mo-C steel systems at secondary aging temperatures. Up to 2 wt% Cr was shown to shift the secondary hardening to lower temperatures and to promote the rapid coarsening of the M_2C carbide. In the development of AF1410 based structural steels (Ref 9), Machmeier et al. (Ref 10, 11) reported accelerated aging kinetics for increased levels of chromium (2 to 3 wt%) in secondary hardening Fe-Co-Ni-Cr-Mo-C steels. During the secondary hardening reaction, M_2C (molybdenum carbide) forms as needles with hexagonal crystal structure along the cube directions [100] of the ferrite (Ref 12), which is associated with the minimum misfit or lattice strain.

Olson et al. (Ref 13, 14) found that molybdenum forms the M_2C carbide initially at nucleation due to the higher driving force from the molybdenum enrichment. Precipitation of M_2C in AF1410 steel is coherent as needles form along the minimum principal strain direction <100>. Chromium, because of its higher diffusivity, replaces the molybdenum in M_2C as the reaction moves toward equilibrium (Ref 15). The diffusion of chromium in the M_2C carbide affects the aging kinetics, carbide composition, and lattice parameter. Ayer et al. (Ref 16-18) showed experimentally that an increase in chromium will decrease the cementite stability and promote the early formation of M_2C carbides. The composition increase in M_2C, with chromium additions, results in lowered molybdenum content, which decreases the carbide/matrix coherency, resulting in lower strength. Transmission electron microscopy by Ayer and Machmeier (Ref 16, 17) revealed, at the peak hardening temperature of 482 °C, M_2C carbides in the 2Cr and 3Cr steels were coherent as evidenced by the black-white strain contrast. Combinations of chromium additions and varying aging temperatures revealed that the loss of coherence and the appearance of fringes were associated with overaging.

While a fundamental understanding of the critical mechanism and microstructural features, which resulted in the high combinations of strength and toughness in AF1410 based steels exists, to some extent, it is acknowledged that a general study of principles is still warranted. Therefore, this investigation is intended to provide an understanding of the secondary hardening phenomenon in the AF1410 based steels at the engineering level. Data from developmental AF1410 based steels, at two chromium levels, were used to investigate this unique behavior over a large range of aging temperatures and times that may be encountered during commercial thermal treatment and/or welding.

2. Experimental Procedure

The steel compositions investigated in this study are listed in Table 1. The 2Cr (AF1410) and 3Cr steels were vacuum induction melted (VIM) and cast into 136 kg ingots, reduced to slabs, and cross rolled to 13 mm plate. All test specimens were removed in the L-T plate orientation.

Specimen blanks were double austenitized at 850 and 801 °C for 1 h with a water quench at each interim. The aging stud-

P.M. Machmeier and **T. Matuszewski,** Snap-on Tools Inc., Kenosha, WI, USA; **R. L. Jones,** R&J Consulting, Fort Worth, TX, USA; **R. Ayer,** STEM, Woodridge, CT, USA.

ies were conducted in a range of temperatures from 200 to 650 °C at times from 0.1 to 100 h.

Tensile tests were conducted at room temperature in accordance with ASTM E 8–95a using a 6.4 mm diam round specimen at a strain rate of 0.003 s^{-1}. Notched single end bend (SEB) (10 × 10 × 55 mm) specimens were used to determine the absorbed energy in a Riehle impact machine (Wilson Instruments, Div. of Instron Corp., Canton, MA) at ambient temperature per ASTM E 23-94b.

The microstructure was determined from 2.3 mm diam thin foils, which were chemically thinned and electropolished in a chromic-acetic acid solution. Transmission electron microscopy (TEM) of the thin foils was accomplished by bright field, dark field, and diffraction techniques.

X-ray diffraction analyses were conducted to determine the volume percent of retained/reverted austenite and the lattice parameters of the martensite matrix at various thermal treatment conditions. The volume percent γ was determined on mechanically and electropolished surfaces by measurement of integrated diffraction intensities using the direct comparison method per ASTM E 975. The standard reference material was NBS No. 485, in which the volume percent austenite was certified to be 3.8 ± 0.2%.

The lattice constants of the martensite (ferrite) unit cell were measured with chromium Kα radiation. The diffraction peaks used in calculating the lattice parameter corresponded to the (110), (200), and (211) planes. In all samples,

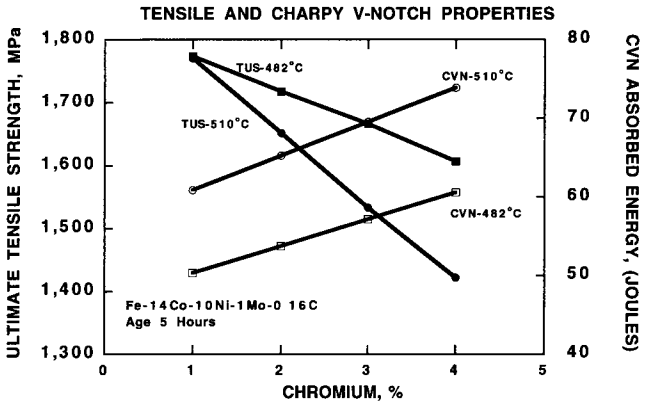

Fig. 1 Effect of Cr on tensile and impact properties of Fe-14Co-10Ni-1Mo-0.16C steels (from predictive equations)

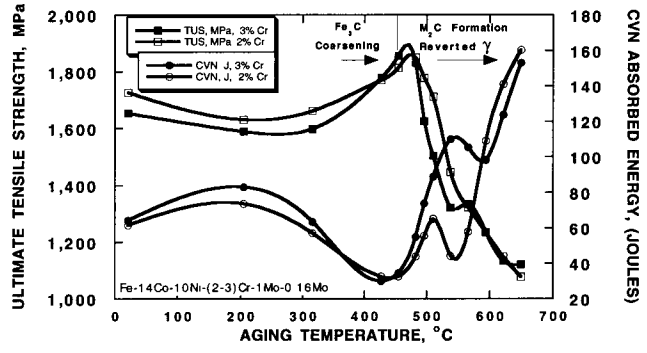

Fig. 2 Effect of Cr on aging response and strength/toughness properties

there was no peak splitting, indicating little deviation from tetragonality($c \approx a$).

The electrical resistivity was measured at ambient temperature on (5.08 × 3.94 × 85.75 mm) specimens, which were quenched and then aged for various times. A collinear four-point probe was applied at 2.83 kg load, where the distance between the potential and current probes was 59.94 and 76.20 mm, respectively. A constant current source of 1 A was used for the measurements and the direct current (dc) voltages were measured to a sensitivity of ±1 μV.

With the current flowing in one direction (forward), the potential drop across the test specimen was measured. Then the direction of the current was reversed, and the potential drop was measured again. Thus, the average value of resistance (R_{avg}) was measured for each run:

$$R_{avg} = \frac{1}{2}(R_f + R_r)$$

Potential drops were measured as a function of current and time to determine errors in measurement and possible heating effects in the specimen. Only very little heating occurred in a specimen carrying 3 A current for 1 h. Currents used in the actual experiments were 1 A or less; thus, very little heating occurred during the time of measurement.

In the development of the AF1410 based series of steels (Ref 10, 11), the use of factorial analysis in experimental designs disclosed that chromium could significantly alter the tensile strength and Charpy V-notch (CVN) absorbed energy. Machmeier et al. (Ref 10), using multiple linear-regression equations derived from the experimental design, where estimates of the individual and synergistic effects of chromium on variables were determined, shows the trend lines for increases in Fig. 1.

3. Results and Discussion

3.1 *General Mechanical Properties*

The AF1410 based 2Cr and 3Cr steels represent a secondary hardening system where high levels of strength are achieved concomitant with increasing toughness. The high strength and toughness can only be achieved if the high dislocation density, which serves as a nucleation site for the M_2C carbide, can be preserved at the normal secondary hardening temperature range. The mechanical property curves for these steels reveal high levels of tensile strength and notch toughness following the double austenitization and quench thermal treatments. Aging up to 200 °C resulted in an increase in yield strength and notch toughness accompanied by a decline in tensile strength (Fig. 2). A further increase in aging temperature resulted in further increases in both yield and tensile strength at the expense of toughness until the onset of the M_2C formation at approximately 458 °C. As the M_2C carbide is precipitated simultaneously with the dissolution of cementite, the strength and toughness are progressively increased until overaging occurs. The 3Cr steel displays slightly lower strength but gives higher toughness during the cementite precipitation. At maximum strength, there is a peak shift of approximately

50° followed by a substantial increase in notch toughness in 3Cr. However, the optimum balance of strength and toughness in the normal aging range favored the 2Cr composition at this carbon level (Ref 10).

3.2 *Structure-Property Relationships*

3.2.1 As-Quenched

The 2Cr steel (Fe-14Co-10Ni-2Cr-1Mo-0.16C) alloy, when water quenched from austenitizing temperatures, revealed a highly dislocated lath martensite with small amounts of twinning and retained austenite (Fig. 3). Due to the high martensite start (M_s) temperature (635 to 665 °C), autotempering of the lath martensite occurred during rapid cooling. In the 2Cr steel, the autotempered precipitates were identified as fairly coarse (110) Widmanstätten Fe_3C carbides, while in the 3Cr steel, the small carbides appear to be dislocation nucleated. The 1 wt% Cr addition (3Cr steel) is effective in retarding autotempering, thus increasing the twinning and increasing the interlath reverted austenite to 1 to 2 vol%.

3.2.2 Iron Carbide Precipitation

In the aging temperature range of 350 to 450 °C, a dramatic loss in impact toughness is noted in Fig. 2 and 4 as cementite coarsens at interlath and twin boundary sites (Ref 9, 16, 19). It was reported that cementite interlath boundary films (Ref 16) exist in the 2Cr, AF1410 steel, indicating that the reverted austenite has transformed in situ. Cementite at the boundary interfaces provides easy crack initiators at moderate strains that coalesce for preferred fracture paths (Fig. 5, 6). The coarsening rate of Fe_3C carbides is controlled by the diffusion of chromium and not necessarily by the self diffusion of iron or diffusion of carbon. This is evident as the increase in chromium promotes the early dissolution of cementite as shown by the wavy carbide interfaces or the absence of Fe_3C at aging temperatures, >450 °C (Fig. 5, 6).

3.3 *Secondary Hardening Reaction*

3.3.1 M_2C Formation

In the aging range from 450 to 510 °C, fine M_2C carbides heterogeneously nucleate at dislocation sites from a supersatu-

Table 1 Chemical composition of Fe-Co-Ni-Cr-Mo-C steels

	Element, wt %											
Alloy	Co	Ni	Cr	Mo	C	Al	Si	Mn	Ti	S	P	O
2%Cr	13.80	10.15	1.95	0.98	0.16	0.009	0.04	0.06	0.01	0.003	0.001	0.0009
3%Cr	13.74	10.02	2.97	1.21	0.16	0.01	0.04	0.16	0.003	0.003	0.007	0.0018

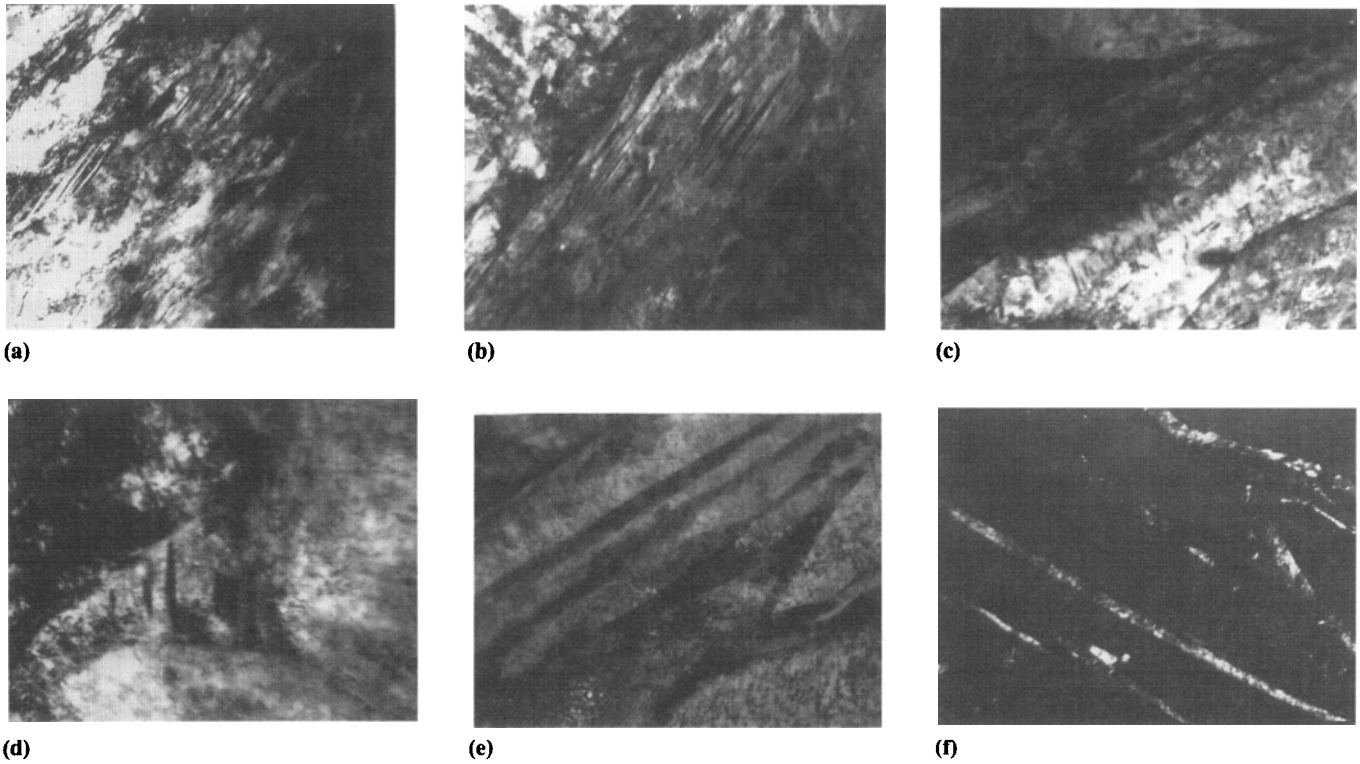

Fig. 3 Effect of Cr on the as-quenched microstructure in Fe-14Co-10Ni-1Mo-0.16C steels. (a) 2%Cr steel, moderate accommodation twinning 20,000×. (b) 3%Cr steel, increase in (112 twinning) 20,000×. (c) 2% Cr steel, auto-tempered carbides identified as (110) Widmanstätten Fe_3C, 20,000×. (d) 3%Cr steel, fine auto-tempered carbides that apparently are dislocation nucleated, 80,000×. (e) 3%Cr steel, light field, 1 to 2 vol%, 40,000×. (f) 3%Cr steel, dark field, retained austenite, 40,000×.

rated matrix (Ref 13, 14, 19). At peak hardness, there is evidence that the small aspect M_2C carbides are coherent with the matrix when precipitated in the <100> direction, the direction of minimum distortion (Ref 16, 19, 20), where the carbide composition varies as $(Mo_{1-x}Cr_x)_2Cy$. The role of chromium in the M_2C carbide during the secondary hardening reaction is quite unique. Chromium increases the propensity for redissolution of cementite and replaces molybdenum in M_2C, thus reducing the size of the carbide during the aging process (Ref 16, 19, 21). The partitioning of chromium between these two reactions accounts for the rate of Fe_3C dissolution in the 2Cr and 3Cr steel at 482 to 510 °C in Fig. 5 and 6. The 3Cr steel at a 482 °C age reveals considerably less Fe_3C than the 2Cr steel. At 510 °C, the cementite is almost nonexistent. The significance is that the increase of 1 wt% Cr shifts the hardening peak to a lower aging temperature (Fig. 4).

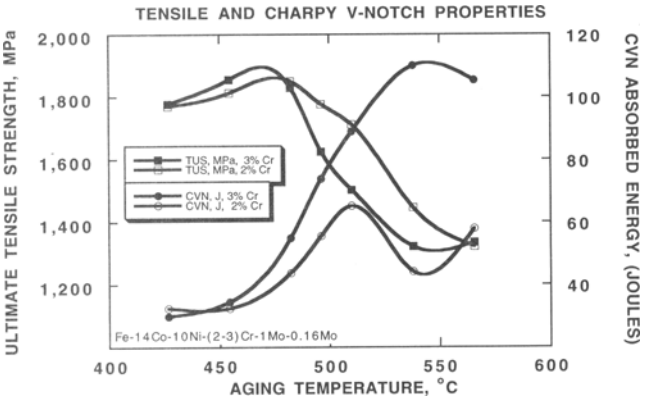

Fig. 4 Strength and toughness relationships during the normal aging range

Two explanations for the peak hardness shift as a function of chromium increase are:

- From electron microscopy results, Ayer et al. (Ref 4, 5, 17, 20) showed streaking along the <001> directions of the martensite, indicative of coherency and the growth direction of M_2C needles. The loss of precipitate and matrix co-

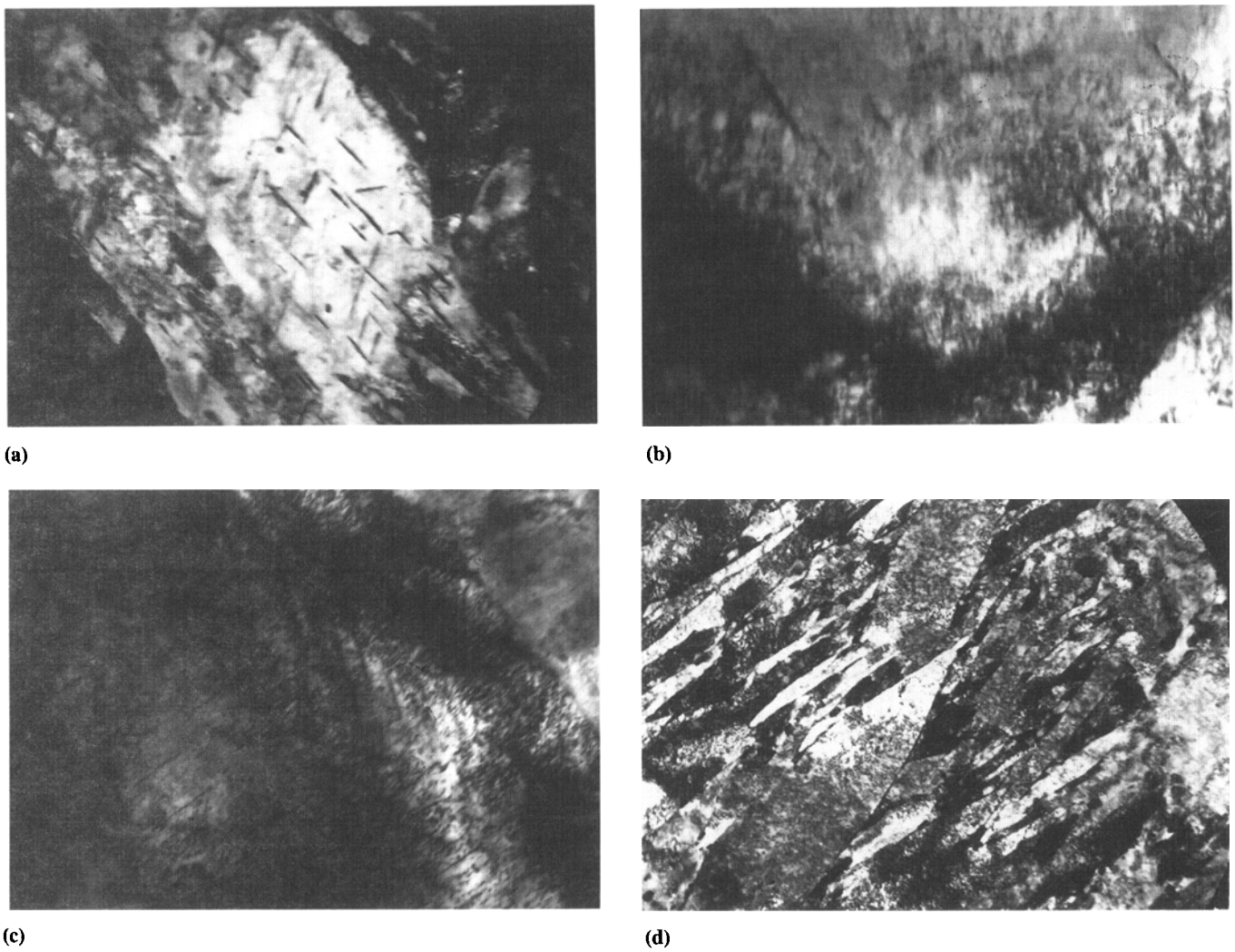

Fig. 5 Microstructural aging progression with 2%Cr: Fe-14Co-10Ni-1Mo-0.16C steel. (a) 427 °C age 5 h, coarse Widmanstätten cementite, 20,000×. (b) 482 °C age 5 h, dissolving cementite carbides M_2C carbide precipitation, 60,000×. (c) 510 °C age 5 h, partial resolution of cementite $(Mo,Cr)_xC$ carbide formation, 40,000×. (d) 538 °C age 5 h, partial recovery, reverted austenite, overaged carbides, 22,000×.

herency, associated with black-white contrast images, occurred during a slight overaging of the M_2C precipitate. This occurs earlier in aging in the 3Cr as chromium progressively replaces molybdenum in the $(Mo,Cr)_2C$ precipitate, increasing the coarsening kinetics and resulting in the coherency loss (Ref 13, 14, 16).

- At peak hardness, the critical precipitate size for the shear stress balance between precipitate shear and Orowan looping is dependent on chromium. The strengthening of these alloys at peak hardness results from the Orowan bypass mechanism because the diffusion of chromium to the M_2C carbide shifts the critical precipitate size to a high value for the 3Cr steel (Ref 13, 16, 21).

At aging temperatures slightly higher than the peak hardening temperatures, overaging for each alloy occurs that involves increased coherency loss, $(Mo,Cr)_2C$ carbide growth, and some recovery of the substructure (Fig. 4, 5). The optimum balance of strength and toughness, conducive to a structural steel of the 2Cr and 3Cr compositions, occurs at 483 and 510 °C, respectively (Fig. 4). Both these aging temperatures are slightly above the peak hardening temperature but balance the property dependent microstructures as: the M_2C coherency strains with the coarsening rate, the degree of cementite dissolution, and the increase in reverted austenite.

3.4 *Toughness Phenomena*

Tensile ductility and impact notch toughness are strongly affected by microvoid nucleation at inclusions and secondary grain refining dispersion and microstructurally formal particles and phases (Fig. 2, 7) in the normal aging range. The large ef-

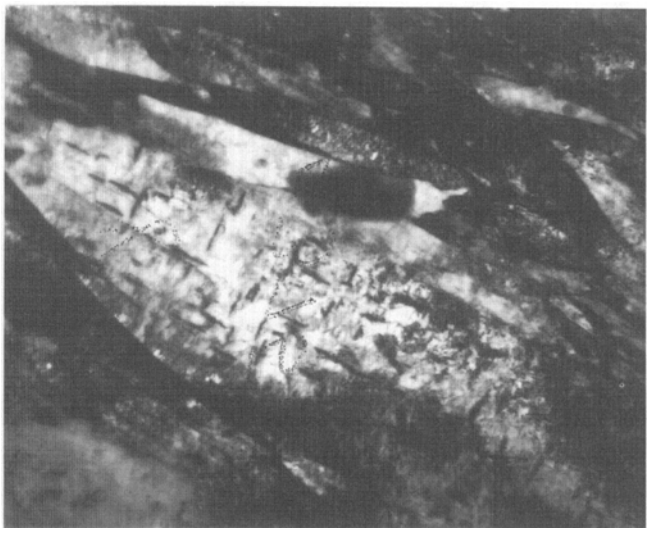

(a)

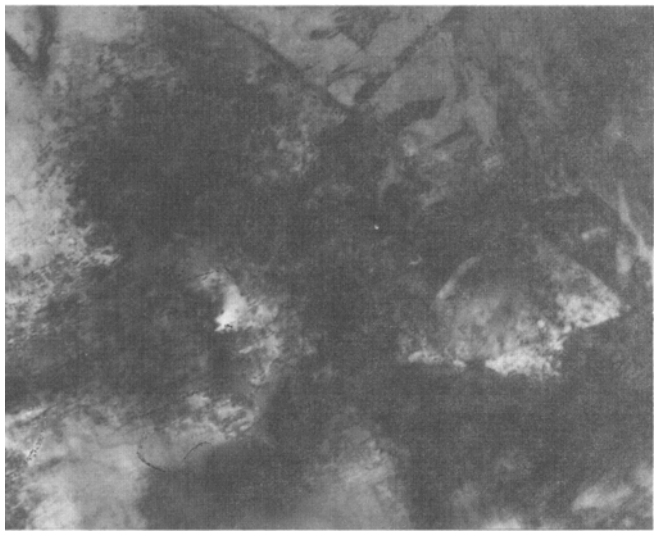

(b)

(c)

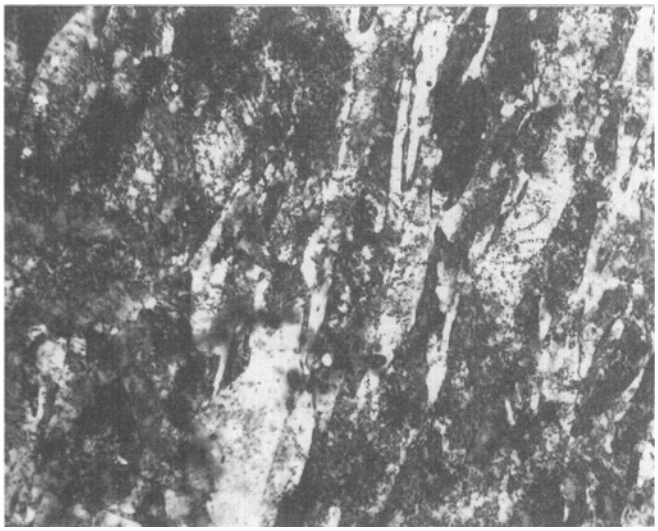

(d)

Fig. 6 Microstructural aging progression with 3%Cr: Fe-14Co-10Ni-1Mo-0.16C steel. (a) 427 °C age 5 h, Widmanstätten cementite, 20,000×. (b) 482 °C age 5 h, Widmanstätten carbides resolutioned, unresolved M_2C type carbides, 60,000×. (c) 510 °C age 5 h, $(Mo,Cr)_xC$ carbides, 40,000×. (d) 538 °C age 5 h, partial recovery, reverted austenite, overaged carbides, 22,000×.

fect of inclusions and dispersoids has been discussed for 2Cr steel (AF1410) using the Needleman model as a criteria (Ref 20, 21). These studies revealed the toughness improvements possible by low impurity melt practice by controlling the shape, size, and spacing of inclusions and their effect on strain-induced particle debonding during deformation (Ref 22, 23).

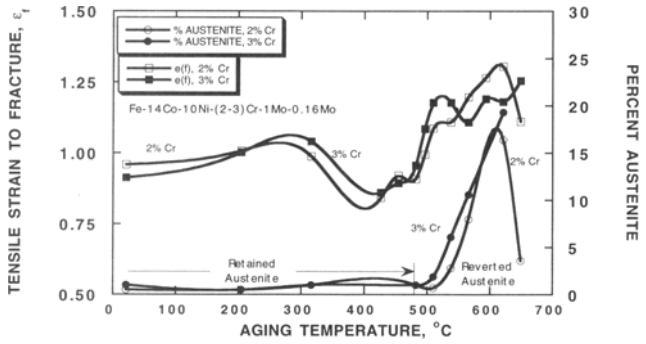

Fig. 7 Relationship between strain to fracture and austenite content

In the following discussion, the emphasis is on thermally controlled microstructures and the effect on toughness. Aging at 204 °C produced an increase in CVN toughness and later an increase in tensile ductility (Fig. 2, 7). At progressively higher aging temperatures up to 427 °C, the tensile yield and ultimate strength both increase while toughness decreases. During the development of the AF1410 steel (Ref 10, 11), Machmeier et al. noted a fracture appearance transition. The dimpled rupture present at 204 °C gradually reverted to low energy fracture mechanisms up to temperatures of 427 °C. The low-toughness fractures showed evidence of a partial change in mechanism from void coalescence to quasi-cleavage at interlath and interpacket and grain boundaries due to the formation and growth of Fe_3C at these sites. The predominant carbide in Fig. 5 and 6 was identified as interlath orthorhombic cementite, which exhibited a definite $(110)_M$ habit plane (Ref 10, 16). In contrast, aging at 482 °C increases the strength properties to maximum values with partial restoration of notch toughness as the transition Fe_3C phase begins to progressively blend into the solution (Ref 10, 11, 16, 19). At 454 °C, the toughness differences between the 2Cr and 3Cr steels is the increased dissolution of the inter-

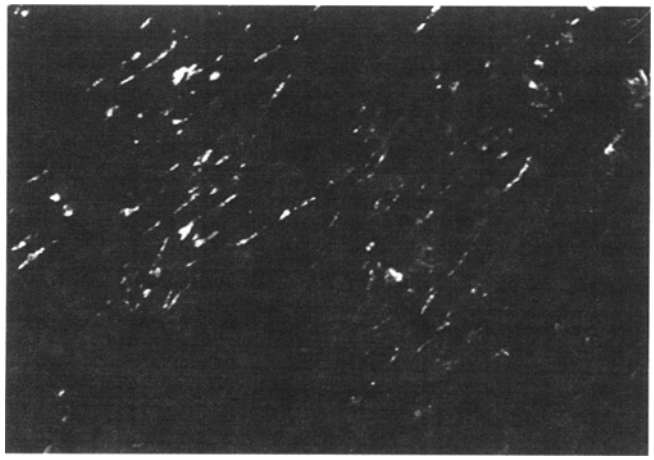

(a)

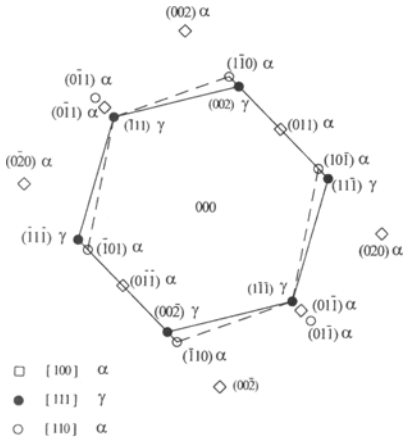

(b)

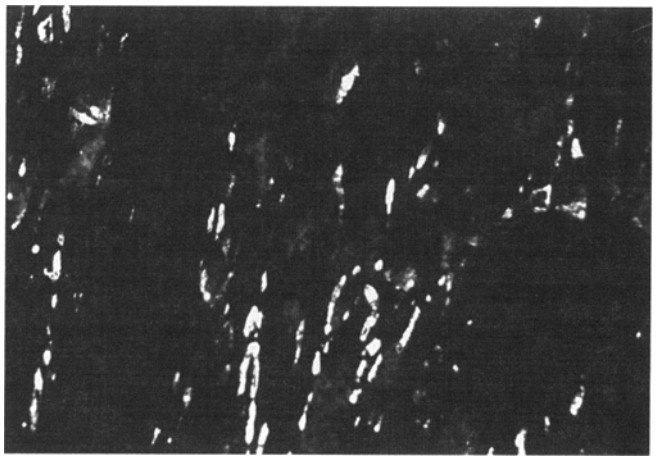

(c)

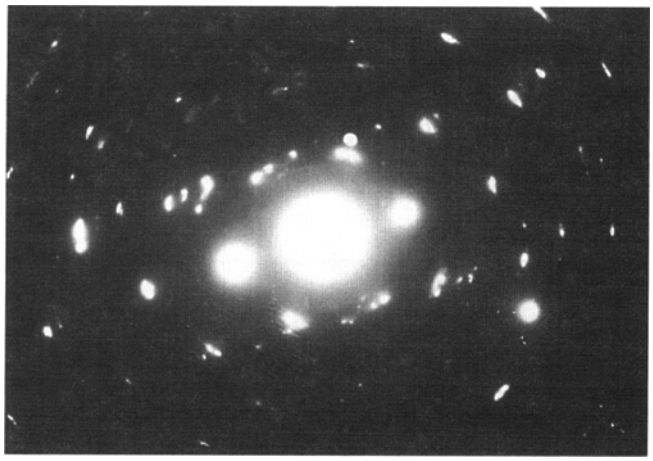

(d)

Fig. 8 Effect of Cr on the precipitation of reverted austenite. (a) 2%Cr alloy, 538 °C age 5 h, 2.8 vol%, reverted austenite, dark field, 22,000×. (b) 3%Cr alloy, 538 °C age 5 h, 6.1 vol%, reverted austenite, dark field illumination, 22,000×. (c) K-S orientation $(01\bar{1})\alpha//(1\bar{1}1)\gamma$ and $(111)\alpha//(110)\gamma$. (d) 510 °C age at 5 h, 2%Cr 0.7-1.0 vol%γ, 3%Cr 1.9 vol%γ.

lath cementite in the latter. The relatively higher toughness of the 3Cr steel at 482 °C was reported again to be the effect of cementite dissolution due to the reverted austenite formation (Ref 16). Thomas (Ref 24) initially demonstrated the beneficial effect of retained austenite on steel toughness even when the austenite formed at interlath sites.

The reverted austenite is relatively stable at high mechanical strains and may assist high toughness fracture by crack blunting. The reverted austenite, identified with a Kurdjumon-Sachs orientation relationship between γ and α' increased from 1.9 vol% at 510 °C to 6.1 vol% at 538 °C for the 3Cr steel (Fig. 7, 8). In the 2Cr steel, the austenite increased from <1.0 to 2.8 vol% over the identical temperature range. At high quantities of reverted austenite, this phase forms as thin interlath films and also at intralath sites as modules (Fig. 8).

3.5 *Physical Properties*

Changes in electrical resistivity can be a useful method to evaluate the hardening response concomitant with the kinetics of aging. In these experiments, the lattice potential of interest is the removal of chromium and carbon atoms from solid solution. The assumptions are that the dislocation density, the impurity level, and aging temperature variances will produce negligible effects where resistivity differences are measured.

The effect of aging response on the 2Cr and 3Cr steel as-quenched microstructures, as measured by hardness and resistivity, is exhibited in Fig. 8. Following the double austenitize and water quench treatment, the formation of fairly coarse autotempered Fe_3C was reported in the 2Cr steel (Fig. 3). The amount of carbon removed from the martensite matrix remained relatively constant over a large aging temperature range. In the peak hardening range, this plot indicates that the resistivity variances may be due to the effects of chromium on the carbide formation. When the resistivity data is normalized at an aging temperature (427 °C), where cementite is the predominant carbide, a substantial variance in resistivity exists between the 2Cr and 3Cr steels as chromium is apparently involved in the carbide reactions (Fig. 9). Because the M_2C carbide exhibits substantial driving force at nucleation, it is postulated that the carbide is initially molybdenum rich, and chromium is then progressively increasing in the $(Mo,Cr)_2C$ carbide as the reaction is completed (Ref 13, 15, 21). The large resistivity drop for the 2Cr steel in Fig. 10 may be the removal of substantial chromium from solution during the increase in aging time from 1 to 5 h. Even at 1 h age time at these temperatures, it is thought that the primary carbide is still Fe_3C with substantial nucleation of molybdenum rich M_2C clusters and carbides; aging at 5 h would increase the chromium partitioning in the M_2C carbide. Early investigations (Ref 11) of the lattice parameter for the two steels revealed substantial differences at the 483 to 510 °C peak hardening age (Fig. 11). While both steels exhibited similar lattice parameters at peak hardening, the 3Cr steel is slightly overaged at 510 °C; thus there is a loss in coherency and an increase in chromium in the $(Mo,Cr)_2C$ carbide. Recent studies (Ref 13, 14, 21) have shown that as chromium replaces molybdenum in M_2C, the size of the M_2C carbide is reduced (smaller lattice parameter) resulting in a correspondence to the ferrite lattice parameter.

3.6 *Aging Kinetics*

Electrical resistivity can be a sensitive monitor of the progress of the status of the aging reactions. However, due to the complex reactions and diffusion variables, it can only be used as a thermal treatment guide with the data in an unmodeled format. Resistivity measurements were started at the as-quenched condition with the first data point appearing at 0.1 h. This was a limitation of the bulk specimens, which are comparable with mechanical property data.

As discussed, resistivity variations are primarily due to carbon and chromium being removed from the martensitic matrix. Analysis of the kinetic aging response of the 2Cr and 3Cr steels in Fig. 12 and 13 reveal that overaging generally occurs at progressively faster response times as the age temperature is increased. During the age at 454 and 482 °C, a small resistivity differential exists between the two steels, even when it is known that 3Cr affects the kinetics of the Fe_3C precipitation and causes the early precipitation of a chromium lean $(Mo,Cr)_2C$ carbide during aging at 482 °C. The aging curves at 510 °C differ strongly in behavior for the 2Cr and 3Cr steels when aged from 1 to 10 h. The 2Cr steel exhibited a sharp decline in resistivity at a 5 h age, while the 3Cr steel exhibited an increase in resistivity. While it is known that chromium reaches

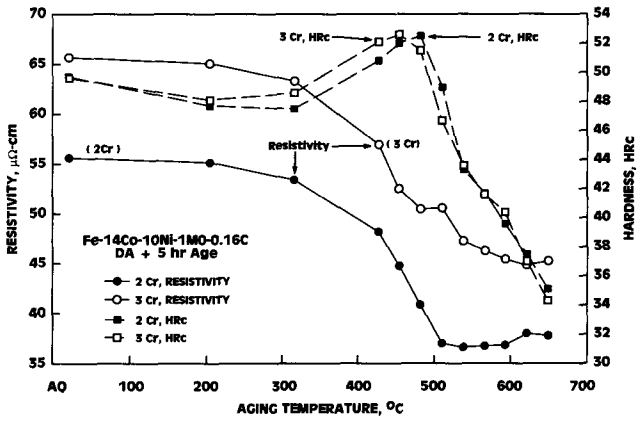

Fig. 9 Variation in resistivity and hardness with aging temperature

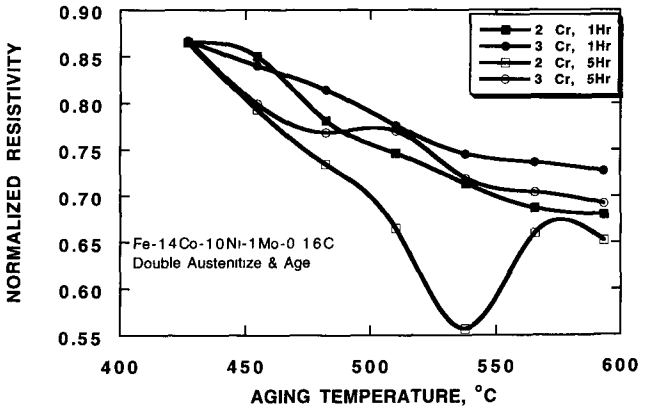

Fig. 10 Effect of aging parameters on resistivity at two Cr levels

a higher value in the $(Mo,Cr)_2C$ carbide in the slightly overaged 3Cr steel, it is the ≈1 vol% differential in reverted austenite that may explain this behavior (Fig. 8). The 2Cr steel exhibited expected behavior as the partitioning of chromium in the M_2C would revert in a leaner chromium martensitic matrix. A precipitous drop in resistivity is evident in Fig. 12 and 13 for both steels when overaged at 621 °C, which results in a substantial recovery, rapid carbide coarsening that depletes the matrix of chromium and carbon, and the rapid increase in reverted austenite.

The hardening responses of the AF1410 based 2Cr and 3Cr steels, as measured by the yield strength over age time, are shown in Fig. 14. The secondary hardening reaction occurs for shorter times with progressively high aging temperatures and increasing chromium content. Also, the peak strength is consistently higher for the 2Cr steel than recorded in the 3Cr composition. Since the peak hardness or yield strength has been shown to be related to very small Cr-lean M_2C carbides, it is expected that the 3Cr steel would exhibit overaged behavior. This results in reduced peak strength and an overaging response to a common strength value for the two steels. A higher Mo $(Mo,Cr)_2C$ carbide seems to be more effective in hardening and in retardation of overaging (Fig. 13). An activation energy relationship was derived from hardness data over the normal aging range for the Fe_3C (52-53 HRC) and the M_2C (48-49 HRC)

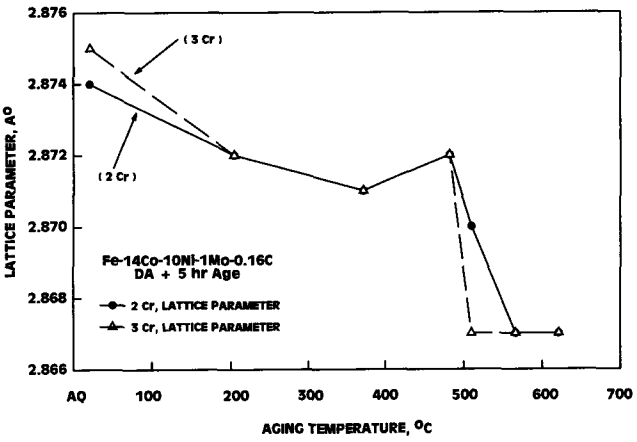

Fig. 11 Variation in lattice parameter with aging temperature

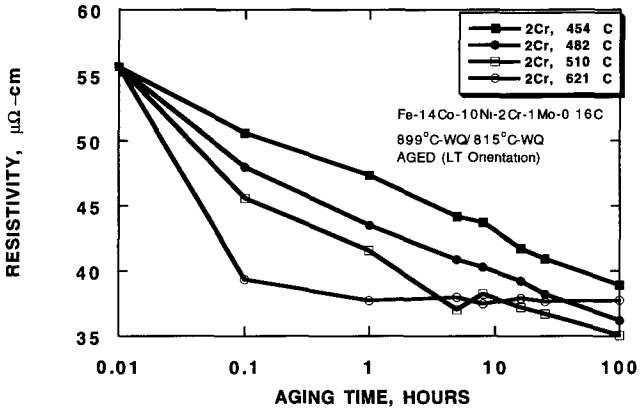

Fig. 12 Aging kinetics in the 2Cr steel

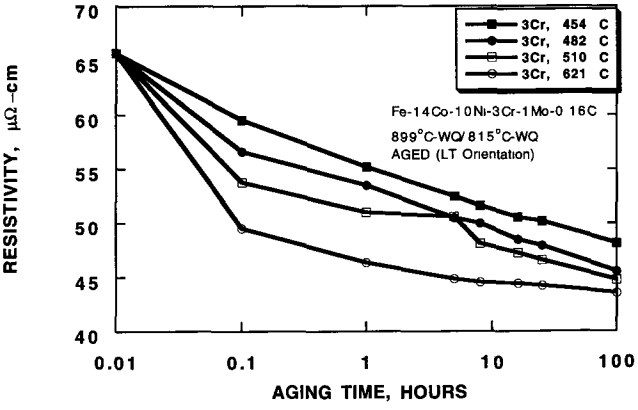

Fig. 13 Aging kinetics in the 3Cr steel

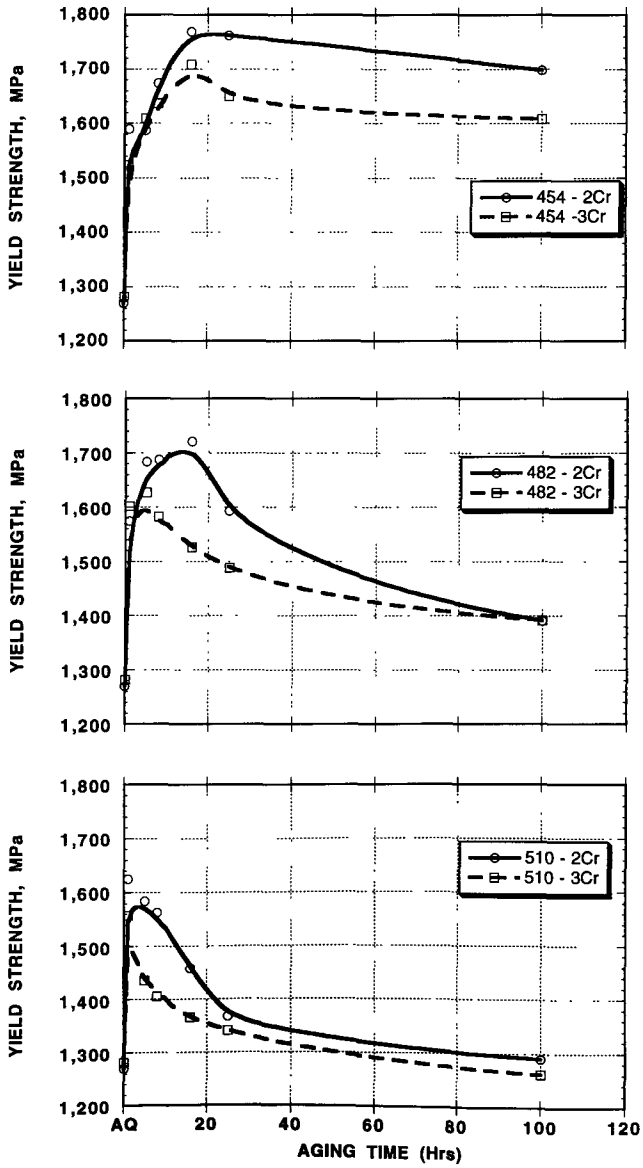

Fig. 14 Effect of Cr on the yield strength aging response

carbide formation regimes (Fig. 15). Although the simultaneous dissolution of Fe_3C and the formation of M_2C is too complex to be accurately studied by hardness alone in this narrow aging rate, estimates of activation energy were determined (Fig. 15). The activation energy (59.5 kcal/g-mole) in the formation of the M_2C alloy carbide, agrees well with the diffusion rates of the diffusing species, Cr (57.3 kcal/g-mole) and Mo (53.9 kcal/g-mole) in α iron (Ref 24).

A possible reason for the agreement of activation energy response at 48-49 HRC is that at 454 to 538 °C, the hardness of specimens aged at 1 to 100 h represented the $(Mo,Cr)_2C$ carbide in the particle coarsening regime. However, the higher peak hardness data (52-53 HRC) represents the formation/dissolution of Fe_3C, M_2C nucleation and M_2C particle coarsening resulting in segmented activation energies higher than predicted for the diffusion of chromium, molybdenum, and carbon in iron. Murphy and Whiteman (Ref 26), in the kinetic study of Mo_2C precipitation in martensite, also reported higher than expected activation energy (83 kcal/g-mole), at all fractions of transformation. It is suggested that in the 454 to 482 °C range, nucleation of M_2C carbides at substructure dislocation sites occur following a long aging exposure.

4. Conclusions

- An increase in chromium from 2 to 3% in the AF1410 steel resulted in a substantial strength decrease concomitant with an increase in toughness during aging in a narrow range of 482 to 550 °C. This behavior is related to a peak hardening shift, early M_2C carbide coarsening, and an increase in reverted austenite for a 1 wt% increase in chromium.
- In the as-quenched condition, both the 2Cr and 3Cr steel microstructures consisted of highly dislocated martensite laths in packet morphology with retained austenite, twinning, and autotempered carbides. A higher content of chromium resulted in an increase in retained austenite, accommodation twinning, and a retardation of coarse cementite autotempered carbides.
- During aging, the 1 wt% chromium increase resulted in a faster dissolution of Fe_3C, a peak hardness shift, a $(Mo_2Cr)_2C$ carbide coherency, particle coarsening, and an increase in reverted austenite. The strength related phenomena is related to the rapid changes in chromium partitioning in the $(Mo,Cr)_2C$ carbide, resulting in a coherency loss and decrease in lattice parameter. An increase of chromium in the AF1410 steel strongly controls the kinetics of the secondary hardening aging reaction as measured by resistivity changes.

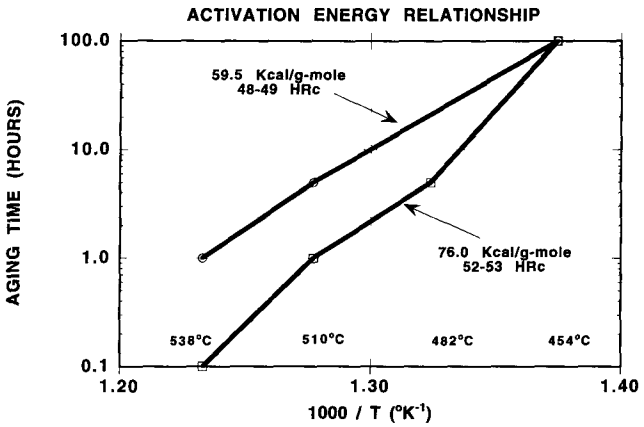

Fig. 15 Activation energy relationship for the aging of Fe-14Co-10Ni-2Cr-1Mo-0.16C steel

References

1. K.J. Irving, The Development of High-Strength Steels, *JISI*, 1962, p 820
2. C.R. Simcoe, A.E. Nehrenherg, V. Biss, and A.P. Coldren, Relationship Between Microstructures and Mechanical Properties on Tempering a Mo-W-V Alloy Steel, *Trans. ASM*, Vol 61, 1968, p 884
3. D. Raynor, J.S. Whiteman, and R.W.K. Honeycombe, In-Situ Transformation of Fe_3C to Mo_2C in Iron-Molybdenum-Carbon Alloys, *JISI*, 1966, p 1114
4. J.J. Irani and R.W.K. Honeycombe, Clustering and Precipitation in Iron-Molybdenum-Carbon Alloys, *JISI*, Vol 203, 1965, p 826
5. D.M. Davies and B. Ralph, Field-Ion Microscopic Study of Quenched and Tempered Fe-Mo-C, *JISI*, 1972, p 262
6. V.K. Chandhok, J.P. Hirth, and E.J. Dulis, "Effect of Cobalt on Tempering Tool and Alloy Steels," *Trans. ASM*, Vol 56, 1963, p 677
7. V. Chandhok, J.P. Hirth, and E.J. Dulis, Effect of Cobalt on Carbon Activity and Diffusivity in Steel, *Trans. AIME*, Vol 224, 1962, p 858
8. G.R. Speich, D.S. Dabkowski, and L.F. Porter, Strength and Toughness of Fe-10Ni Alloys Containing C, Cr, Mo and Co, *Metall. Trans.*, Vol 4, 1973, p 303
9. C.D. Little and P.M. Machmeier, "High Strength Fracture Resistant Weldable Steels," U.S. Patent 4,076,525, 1978
10. P.M. Machmeier, C.D. Little, M.H. Horowitz, and R.P. Oates, Development of a Strong (1650MN/m^2 tensile strength) Martensitic Steel Having Good Fracture Toughness, *Met. Technol.*, 1979, p 291
11. C.D. Little and P.M. Machmeier, "Development of a Weldable High Strength Steel," Report AFML-TR-75-148, AFML, WPAFB, 1975
12. D.J. Dyson, S.R. Keown, D. Raynor, and J.A. Whiteman, The Orientation Relationship and Growth Direction of Mo_2C in Ferrite, *Acta Metall.*, Vol 14, 1966, p 867
13. G.B. Olson, Overview: Science of Steel, *Innovation in Ultrahigh Strength Steel Technology*, Proc. 34th Sagamore Army Materials Research Conference, G.B. Olson, M. Azrin, and E.S. Wright, Ed., U.S. Army Materials Technology Laboratory, Watertown, MA, 1990, p. 3
14. J.S. Montgomery, G.B. Olson, *Innovation in Ultrahigh Strength Steel Technology*, Proc. 34th Sagamore Army Materials Research Conference, G.B. Olson, M. Azrin, and E.S. Wright, Ed., U.S. Army Materials Technology Laboratory, Watertown, MA, 1990, p 147
15. G.B. Olson, T. J. Kinkus, and J.S. Montgomery, APFIM Study of Multicomponent M_2C Carbide Precipitation in AF1410 Steel, *Surf. Sci.*, Vol 246, 1991, p 238
16. R. Ayer and P.M. Machmeier, "Microstructural Basics for the Effect of Chromium on the Strength and Toughness of AF1410-Based High Performance Steels," *Metall. Trans.*, Vol 27A, 1996, p 2510
17. R. Ayer and P.M. Machmeier, Transmission Electron Microscopy Examination of Hardening and Toughening Phenomena in Aermet 100, *Metall. Trans. A*, Vol 24, 1993, p 1943
18. Y. Oh, P.M. Machmeier, T. Matuszewski, and R. Ayer, Evaluation of the Nucleation and Growth Kinetic Behavior of the

Secondary Hardening Carbide of Fe-14Co-10Ni-1Mo-0.16C Steels, at Two Cr Levels, Using an Analytical and Modeling Approach: Part II, *J. Mater. Eng. Perform.*, Vol 6 (No. 3), 1997, p 289-299

19. M. Grujicic, Design of M_2C Carbides for Secondary Hardening, *Innovations in Ultrahigh Strength Steel Technology*, ibid., p 223
20. R. Ayer and P.M. Machmeier, Analytical Electron Microscopy Examination of Peak Hardening Phenomena in a Secondary Hardening, Ultrahigh Strength Steel, *Microstructures and Mechanical Properties of Aging Material*, P.K. Liow et al., Ed., The Metals and Material Society, 1993, p 251
21. H.M. Lee, A.J. Garratt-Reed, and S.M. Allen, Composition of M_2C Phase in Tempering of High Co-Ni-Steels, *Scr. Metall.*, Vol 25, 1991, p 685
22. M.J. Gore, G.B. Olson, and M. Cohen, Grain-Refining Dispersions and Properties in Ultrahigh-Strength Steels, *Innovations in Ultrahigh Strength Steel Technology*, ibid., p 425
23. W.M. Garrison and N.R. Moody, The Influence of Inclusing Spacing and Microstructure on the Fracture Toughness of the Secondary Hardening Steel AF1410, *Metall. Trans. A*, Vol 18, 1987, p 1257
24. G. Thomas, Retained Austenite and Tempered Martensite Embrittlement, *Metall. Trans. A*, Vol 9, 1978, p 439
25. P.J. Alherry and C.W. Haworth, Interdiffusion of Cr, Mo, and W in Iron, *Met. Sci.*, Vol 8, 1974, p 349
26. S. Murphy and J.A. Whiteman, The Kinetics of Mo_2C Precipitation in Tempered Martensite, *Met. Sci.*, Vol 4, 1970, p 58